

Engineering Zwitterionic-switchable Chromatin-mimetic Nanoparticles for  
Immune Modulation

Jingyi Xie

A thesis

submitted in partial fulfillment of the requirements for the degree of  
Master of Science

University of Washington

2018

Supervisory Committee:

Shaoyi Jiang, Chair

Kim Woodrow

Program Authorized to Offer Degree:

Bioengineering

©Copyright 2018

Jingyi Xie

University of Washington

Abstract

Engineering Zwitterionic-switchable Chromatin-mimetic Nanoparticles for

Immune Modulation

Jingyi Xie

Chair of the Supervisory Committee:

Shaoyi Jiang

Chemical Engineering & Bioengineering

Currently, one of the major obstacles that impede the wide application of therapeutic protein products is their potential immunogenicity, especially for those obtained from non-human sources. The immune response will decrease the efficacy of protein drugs and lead to adverse events such as anaphylaxis, cytokine-release syndrome, and cross-reactive neutralization of endogenous proteins. This thesis studied an immunosuppressive nanoparticle capable of inducing durable immune tolerance to co-delivered proteins in order to suppress the unwanted immune responses against protein drugs. The formulation of this nanoparticle was developed and optimized to stably encapsulate protein antigens and immunosuppressive nucleotides simultaneously. The stability and degradability of this nanoparticle were also characterized. Moreover, using KLH as a model protein antigen, we demonstrated that the immunosuppressive nanoparticle in mice could mitigate the immune responses against KLH. Collectively, the immunosuppressive nanoparticle developed in this thesis provides a general tool to decrease undesirable immune responses.

## Contents

1. Introduction.....	4
1.1 Undesirable immune responses in biopharmaceutical industry .....	4
1.2 Nanoparticles for immune modulation .....	5
1.3 The immune-tolerance behavior of apoptotic cells .....	6
1.4 Chromatin-mimetic zwitterionic nanoparticle for antigen-specific immune tolerance .....	8
2. Materials.....	11
3. Methods.....	12
3.1 Synthesis of immunosuppressive nanoparticles .....	12
3.2 Characterization of immunosuppressive nanoparticles.....	13
3.3 Stability study.....	14
3.4 Degradation study .....	15
3.5 Animal experiment .....	15
3.6 ELISA .....	16
4. Results and Discussion .....	17
4.1 Size distribution and zeta-potential of immunosuppressive nanoparticles.....	17
4.2 Encapsulation result.....	19
4.3 Stability test .....	23
4.4 Degradation profile .....	24
4.5 Immune modulation result .....	27
5. Conclusions .....	29
6. Reference.....	30

## **Introduction**

### **1.1 Undesirable immune responses in biopharmaceutical industry**

Recently, the US FDA has advocated that the biopharmaceutical industry should take a proactive risk-based approach to reduce and mitigate unwanted immunogenicity(1). Undesirable immune response is a critical consideration in clinical interventions(2). Protein drugs with high potency and specificity have demonstrated promising therapeutic potential. However, many of them are immunogenic eliciting the production of anti-drug antibodies (ADAs), which limit their safety and efficacy(3). Binding of ADAs to protein drugs have been shown to cause non-responsiveness to the specific drugs among patients either by neutralizing their pharmacological activity or diminishing their therapeutic exposure through accelerated blood clearance (ABC). In addition, ADAs can evoke life-threatening adverse reactions such as anaphylaxis, raising serious safety issues.

Factors that may contribute to immunogenicity include product stability and aggregation, the mechanism of action, contaminants, the route of administration, the dose regimen, patient genetics, health status and concomitant medications. Current approaches to reducing the immunogenicity of biologics, such as pegylation, do not work universally. For example, Pegloticase (Krystexxa), a pegylated enzyme used to metabolize uric acid for the treatment of refractory gout, induces ADAs in ~90% of subjects, resulting in the loss of efficacy as well as anaphylactic reactions. Hence, a universal strategy to reduce or eliminate immunogenicity is highly preferred to better exploit the benefits of protein drugs.

## 1.2 Nanoparticles for immune modulation

Induction of antigen-specific immune tolerance with immune modulators is emerging as a new method to address the problem of immunogenicity(4). The achievement of antigen-specific immune tolerance has been a long-standing goal for the treatment of diseases caused by undesirable immune response including autoimmune diseases, allergies, allograft rejection and anti-drug antibody responses.

Nanoparticles have emerged as powerful tools to modulate immune responses due to their inherent capacity to target antigen-presenting cells (APCs) and deliver coordinated signals that can elicit an antigen-specific immune response(5). A wide range of strategies have been described to create immunosuppressive nanoparticles (INPs) that fall into three broad categories. One strategy includes INPs that carry antigen alone to harness natural tolerogenic processes and environments, such as oral tolerance, the tolerogenic environment of the liver, and presentation of antigen in the absence of costimulatory signals. A second strategy includes INPs that carry antigen and tolerogenic receptors, such as pro-tolerogenic cytokine receptors, aryl hydrocarbon receptor, FAS receptor, and the CD22 inhibitory receptor. A third strategy includes INPs that carry a payload of tolerogenic pharmacological agents that can induce APCs into an immature state that favors tolerogenic presentation of antigens. These diverse strategies have led to the development of INPs that are capable of inducing antigen-specific immunological tolerance, not just immunosuppression. Various natural and synthetic polymers have been used for INP manufacturing, including polylactic acid (PLA), poly (lactic-co-glycolic acid) (PLGA), polystyrene, acetylated dextran, poly-l-lysine, polyacrylamide, and chitosan. These novel INPs

technologies indicate a promising approach to specifically prevent and treat unwanted immune reactions in human.

Attempts to induce antigen-specific immune tolerance have been made through co-administration of protein antigens and small-molecule immunosuppressive drugs including rapamycin via INPs such as PLGA(6, 7). Rapamycin is a macrolide compound that suppress the immune response by inhibiting the activation of T cells and B cells and reducing their sensitivity to interleukin-2. It is used for the prevention of transplant rejection, lymphangiomyomatosis, and coronary stent coating(8). However, this small-molecule drug often bear some potential toxicities in addition to their immune suppression effect, which raise safety concerns for its application.(9-11). For example, rapamycin-dependent immunosuppressive method suffers the risk of off-target side-effects since the mechanistic target of rapamycin, mTOR is widely expressed in body. Therefore, a safe and efficient strategy that can specifically suppress unwanted immune response is highly desirable.

### **1.3 The immune-tolerance behavior of apoptotic cells**

Apoptotic cells exhibit immune tolerance as evidenced by the lack of immune response to autoantigens in healthy individuals(12-14). Thus, efforts have been made to take advantage of this effect to trigger antigen specific tolerance for therapeutic purposes. For example, ex vivo coupling of autoantigens to apoptotic cells has been used for treatment of autoimmune diseases(15). This raises the possibility of applying this approach to suppress the immunogenic effects of protein drugs as well. However, the general manufacturing process for ex vivo cell coupling is unfavorably burdensome due to the requirement for uniformity as well as their

limited stability and shelf life. To confront these drawbacks, the development of nanoparticles that resemble apoptotic cells and achieve similar antigen-specific immune-tolerance outcomes is particularly preferred.

Studies indicate that the DNA chromatin complex is one component in apoptotic cells that contributes to their immune-tolerance behavior. During the process of apoptosis, the DNA-chromatin complex is translocated to cell membranes allowing for antigen presenting cells (APCs) to engulf these complexes into endosomes. Thereafter, chromatin degradation releases the DNA, which impedes TLR9, a pattern recognition receptor existent in some classes of APCs(16). TLRs are receptors expressed in immune cells including dendritic cells, macrophages, natural killer cells, and other antigen presenting cells located either on the cell surface or within endocytic vesicles. TLR9, specifically, is expressed in endosomes and plays an important role in immune signaling by increasing pro-inflammatory cytokine production. It is a rapidly evolving area to manipulate the immune response by using TLR9 agonist or antagonist. Inhibition of TLR9 in APCs suppresses the expression of co-stimulatory molecules and, thereby, restrains their maturation. Antigen presentation by immature APCs subsequently prompts the differentiation of T cells into regulatory T cells (Tregs), inducing antigen-specific tolerance.

Congruently, GpG, an oligonucleotide as known the antagonist of TLR9 is expected to rise to similar immune tolerance effects(17-20). As a structural analog of TLR9 agonist CpG, GpG can competitively bind to TLR9 receptor and block the effective signaling for inflammation(21, 22). Importantly, unlike mTOR, TLR9 expression in humans is restricted to B cells and Type I interferon-producing plasmacytoid dendritic cells, suggesting that TLR9 targeting with GpG has



fewer off-target issues while exhibiting similar immunosuppressive effects as rapamycin(23, 24). Therefore, we hypothesize that INPs that simultaneously releases GpG and protein antigens in the endosome of APCs will converts an immunogenic protein to a tolerogenic form by teaching the immune system to accept the protein as self in a way similar to DNA-chromatin complexes.

#### **1.4 Engineer zwitterionic materials as chromatin-mimetic nanoparticle for antigen-specific immune tolerance**

To achieve the delivery of anionic nucleotides and proteins, cationic polymers are required as the vehicle. Cationic NPs are extensively studied in the field of gene delivery, with the higher capability of nucleic acid payload uptake. However, cationic NPs have higher cytotoxicity and show stronger ability to interact with and disrupt the cell membrane. In addition, cationic NPs often aggregate upon interaction with negatively charged albumin in serum. The existing polycations, like poly-L-Lysine (PLL), polyamidoamine dendrimers (PAMAM), and polyethylenimines (PEI) provide various chemical and structural selections. However, these polycations are believed to bear cytotoxicity and cannot adequately release the anionic cargos when the electrostatic attraction between the DNA and the polymer prevents the dissociation. Dissociation is a crucial step for DNA loaded cargo, which allows DNA to enter the nucleus or provide further therapeutic effect. To address these issues, a new switchable cationic polymer, tert-butyl polycarboxybetaine (tbPCB) has been developed by our group(25-27). By hiding the anionic carboxylate group in the carboxybetaine moiety with an ester, tbPCB is cationic in physiological condition. However, intracellular hydrolysis of the ester in the acidic condition will lead tbPCB to PCB, a zwitterionic polymer (Figure 1). Upon hydrolysis, the cationic ester converts to ionic carboxylic acid, which repulse the negatively charged DNA and render the

polymer zwitterionic by electrostatic interaction with the positively-charged amine. Then, a water layer formed by strong hydration around the positive and negative charges will contribute to the ultra-low-fouling effect of zwitterionic PCB.

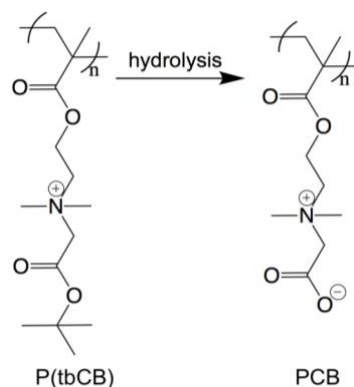


**Figure 1. Scheme of switchable cationic tbPCB.** A zwitterionic polymer PCB is formed upon the hydrolysis of tbPCB.

Zwitterionic materials possess simultaneously oppositely charged ions in the same moiety while maintaining an overall neutral charge. These materials emerged as a class of biomaterials with super-hydrophilic characteristics, mediated by electrostatic interactions between zwitterions and surrounding water molecules. Poly(carboxybetaine) (PCB) is a naturally occurring osmolyte present in humans, animals, and plants, that functions as a protein stabilizer. Our group has conducted extensive research on PCB over the last decades and demonstrated the super-hydrophilicity of PCB polymer and its capacity in eliminating nonspecific protein adsorption, a quality called non-fouling, even in human whole blood (protein adsorption < 0.3ng/cm<sup>2</sup>)(28-30). Also, it was demonstrated that ultra-low-fouling PCB hydrogels do not induce the foreign body response and resist collagenous capsule formation for at least 3 months after subcutaneous implantation in mice(31). Therefore, the conversion of tbPCB to zwitterionic PCB is expected to

facilitate the release of anionic cargos such as nucleotides and proteins due to the non-fouling property of PCB(32). Moreover, the structure of PCB is mainly composed of glycine betaine, a naturally-occurring protein stabilizer present in human body. For humans, the estimated daily intake of glycine betaine ranges from 0.1 to 2.5 g. Such biomimetic property of PCB allows it to owe good biocompatibility and low toxicity.

In this thesis, we developed an immunosuppressive nanoparticle containing GpG and protein antigen. As illustrated in Figure 2, the nanoparticle's scaffold is composed of tbPCB, which is positively charged at physiological pH, favoring nucleotide binding, but reverts to zwitterionic in acidic condition for endosomal release of the nucleotide. Concurrently, the crosslinker glycerol diamethacrylate in the immunosuppressive nanoparticle is acid-degradable such that protein antigens are liberated in the endosome of targeted APCs. A stable formulation of INPs that can simultaneously encapsulate GpG and protein has been optimized and characterized. Moreover, using KLH as the protein antigen for proof of concept, we proved that pre-administration of the immunosuppressive nanoparticle can induce tolerance against KLH in mice for three weeks.

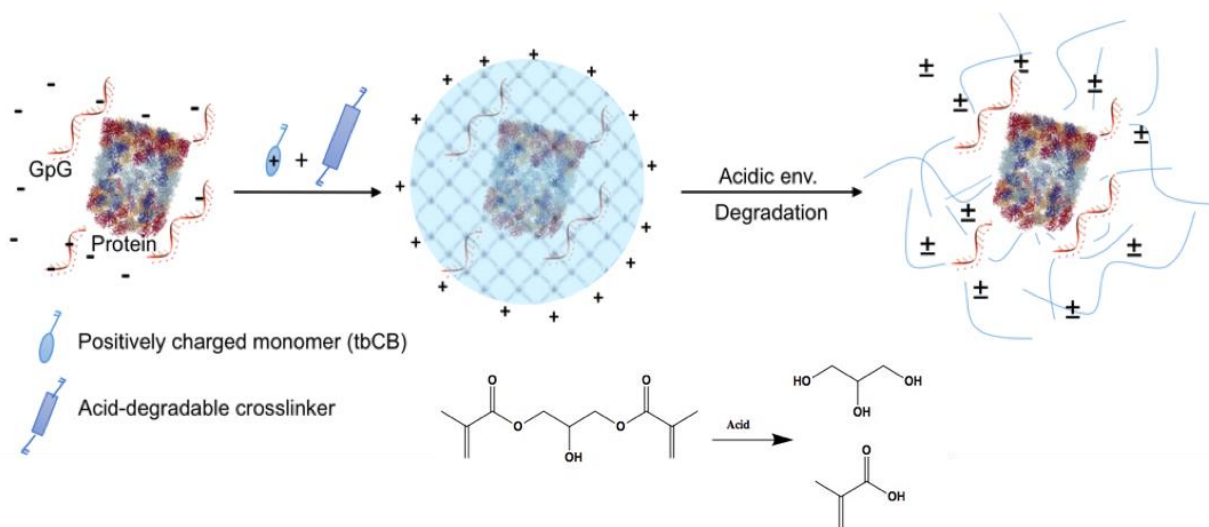


**Figure 2. Scheme of INP formation and degradation.** The positive-charge monomer tbCB is firstly enriched around the negatively-charged GpG and proteins mainly through electrostatic interactions. Subsequent free-radical polymerization wraps proteins and GpG molecules within thin shells of network polymer, forming INPs. The INPs are positively charged at physiological pH for delivery and will revert to zwitterionic under acidic endosomal conditions for unpackaging of GpG. Concurrently, the INPs cross-linker is acid-degradable such that both GpG and protein antigens are liberated in the endosome.

## 2. Materials

All chemicals and proteins including keyhole limpet hemocyanin (KLH) were purchased from Sigma-Aldrich (St. Louis, MO) unless otherwise noted and were used as received.

TLR9 antagonist, GpG (5'-T\*G\*A\*C\*T\*G\*T\*G\*A\*A\*G\*G\*T\*T\*A\*G\*A\*G\*A\*T\*G\*A-3') were synthesized by IDT with a phosphorothioate backbone. Carboxy betaine ester monomer terminated with tbutyl (tbCB) was synthesized following our previously published method. Amicon Ultra centrifugal filter was purchased from EMD Millipore (Billerica, MA). C57LB/6 mice (male, body weight 20–30 g) were purchased from Jackson Laboratories (Seattle, WA). All animal experiments adhered to federal guidelines and were approved by the University of Washington Institutional Animal Care and Use Committee (IACUC). Animals were randomized to treatment groups at the beginning of each study. A sample size of five animals per group was used.

### 3. Methods

#### 3.1 Synthesis of immunosuppressive nanoparticles

To visualize protein on agarose gel, KLH was labeled with Rhodamine dye before being used for INPs preparation. Briefly, KLH was dissolved in  $\text{Na}_2\text{CO}_3$  solution (2 mg/ml, pH 9) and reacted with NHS-Rhodamine 6G solution (50  $\mu\text{L}$ , 100  $\mu\text{g}/\text{ml}$  in DMSO for 2h at room temperature. Unreacted dyes were removed by centrifuge using a Amicon Ultra centrifugal filter (MWCO 10 kDa). GpG (1.5mg/ml), KLH (1.5 mg/mL), acrylamide (AAm) (20%, m/v), tbCB (20%, m/v), and cross-linker glycerol diamethacrylate (GDA) (10%, m/v) were dissolved in PBS buffer (20 mM, pH 7.4).

For the preparation of INP (GpG/KLH), GpG:KLH (G:K) weight ratio was fixed at 8:1. To optimize a formulation that can encapsulate GpG and KLH stably, different INPs were prepared and compared with various monomers:GpG (M:G) ratio (Table 1). For example, to prepare INPs (M:G molar ratio = 3200:1, G:P weight ratio= 8:1), 40  $\mu\text{L}$  GpG (1.5 mg/ml) and 5  $\mu\text{L}$  KLH (1.5 mg/mL), 0.7  $\mu\text{L}$  acrylamide (20%, m/v), 10  $\mu\text{L}$  tbCB (20%, m/v), and 1.8  $\mu\text{L}$  glycerol diamethacrylate (10%, m/v) were added and thoroughly mixed using vortex. The INPs were prepared using free-radical polymerization method. In brief, the mixture of polymer, cross-linker, GpG and protein was added in a 200  $\mu\text{L}$  EP tube. PBS buffer was added to make the final mixture volume to be 100  $\mu\text{L}$ . The polymerization was then initiated by adding 1  $\mu\text{L}$  of ammonium persulfate (APS, 10% m/v) and 4  $\mu\text{L}$  of N,N,N',N'-tetramethylethylenediamine (TEMED, 10% m/v). The reagents were thoroughly mixed by vortex. Cross-linking typically occurs in several minutes, but the reaction was proceeded for 2 hours at 4 °C to achieve maximum encapsulation.

Then free GpG and unreacted monomers and initiators were removed by centrifuge using a Amicon Ultra centrifugal filter (MWCO 100 kDa). The yielded INP were used fresh.

<b>M:G ratio</b>	<b>GpG</b> ( $\mu\text{L}$ )	<b>KLH</b> ( $\mu\text{L}$ )	<b>AAm</b> ( $\mu\text{L}$ )	<b>tbCB</b> ( $\mu\text{L}$ )	<b>GDA</b> ( $\mu\text{L}$ )	<b>APS</b> ( $\mu\text{L}$ )	<b>TEMED</b> ( $\mu\text{L}$ )
<b>6400:1</b>	40	5	1.4	20	3.6	2	8
<b>3200:1</b>	40	5	0.7	10	1.8	1	4
<b>1600:1</b>	40	5	0.35	5	0.9	0.5	2
<b>800:1</b>	40	5	0.18	2.5	0.45	0.25	1
<b>400:1</b>	40	5	0.09	1.25	0.225	0.125	0.5
<b>200:1</b>	40	5	0.045	0.075	0.112	0.075	0.25

**Table 1. Optimize the INPs formulation.** PBS buffer was added respectively and the total volume for polymerization was 100  $\mu\text{L}$ . The M:G ratio was optimized from 6400:1 to 200:1, with a fixed G:K ratio of 8:1.

### 3.2 Characterization of immunosuppressive nanoparticles

The hydrodynamic size and surface zeta-potential of INPs were characterized. DLS and zeta measurements were taken at 173° scattering angle using a Zetasizer Nano instrument (Malvern Instruments, Worcestershire, UK).

Agarose gel electrophoresis was used to test the encapsulation result of INPs. The agarose gel assay was carried out in 2% (w/v) agarose gel at a constant voltage of 100 V for 20 mins. Tris acetate EDTA (TAE) was used as the buffer. To make GpG visible on agarose gel, ethidium bromide (EtBr) was used as a nucleic acid stain here. Briefly, 2 g agarose powder was mixed

with 100 ml 1×TAE buffer in a microwavable flask. The agarose gel was microwaved for 1-2 min in pulses, until the it was completely dissolved. Then allow 1-2 minutes till the agarose gel cool down to about 50 °C. 3 µl EtBr stock solution was added into the agarose solution and mixed to visualize DNA under UV light. Then, the solution was poured into a gel tray with the well comb and placed at 4 °C for 20 mins until it has completely solidified. The gel was then placed into the electrophoresis unit filled with 1×TAE buffer.

Each INPs sample were mixed with loading buffer and loaded into different wells of the gel to provide a visible dye that helps with gel loading and increase the density of sample causing it settle to the bottom of the well. GpG solution and KLH-Rhodamine solution were also mixed with loading buffer. GpG solution and KLH-Rhodamine solution were used as the control and loaded into the last two wells of the agarose gel. The electrophoresis was performed at 100V for 20 mins so that the first band is approximately 75% of the way down the gel. Then the GpG and KLH bands were visualized at 365 nm using a UV gel image system (SIM135A, SIMON).

To optimize the best formulation for encapsulation, INPs with different M:G ratio were prepared and characterized with agarose gel electrophoresis. The agarose wells were loaded with different formulations of INPs: 6400:1, 3200:1, 1600:1, 800:1, 400:1, 200:1, Rodanmin-KLH, and GpG control.

### **3.3 Stability study**

For the stability study, INPs (GpG/KLH) was incubated in 50mM PBS buffer (pH 7.4) and Heparin solution (5mg/ml and 15 mg/ml) at 37 °C. To test the stability of INPs in PBS, we check the agarose gel electrophoresis result after 2 hours. For heparin binding stability study, we

separate INPs into 6 groups. Group 1, 2, 3 were incubated with 5 mg/ml heparin. Group 4, 5, 6 were incubated with 15mg/ml heparin. The incubation time for group 1 and 4 was 30 mins. The incubation time for group 2 and 5 was 1 hour and the incubation time for group 3 and 6 was 2 hours. After the incubation, agarose gel electrophoresis was carried out in 2% agarose gel that contains ethidium bromide in 1×TAE buffer at a constant voltage of 100 V for 20 min. The lanes were loaded with fresh prepared INPs, INPs incubated in PBS for 4 hours, INPs incubated in 5mg /ml heparin for 30 mins, 1hour and 2 hours, INPs incubated in 15mg /ml heparin for 30 mins, 1hour and 2 hours, GpG control, KLH control. Then, the GpG and KLH bands were visualized at 365 nm using a UV gel image system.

### **3.4 Degradation study**

For the degradation study, INPs (GpG/KLH) was incubated in 50 mM sodium acetate buffer (pH 5.4) for 4 hours at 37 °C. To test the effect of polymer content on degradation profile, INPs formulation with M:G ratio of 3200:1 was tested. To get the degradation profile of INPs, we performed agarose gel electrophoresis with different incubation time (0-4 hours). After the incubation, agarose gel electrophoresis was carried out in 2% agarose gel that contains ethidium bromide in 1×TAE buffer at a constant voltage of 100 V for 20 min. The lanes were loaded with fresh prepared INPs, INPs incubated in acid condition for 1 hour, 2 hours, 3 hours, 4hours, GpG control, KLH control. Then, the GpG and KLH bands were visualized at 365 nm using a UV gel image system.

### **3.5 Animal experiment**



All animal experiments adhered to federal guidelines and were approved by the University of Washington Institutional Animal Care and Use Committee (IACUC). C57LB/6 mice (male, body weight 20–30 g) were purchased from Jackson Laboratories (Seattle, WA). Animals were randomized to treatment groups at the beginning of each study. A sample size of five animals per group was used.

Mice were IV. injected weekly with free KLH, PBS, INP#1 (12.5 µg GpG/25 µg KLH), INP#2 (50 µg GpG/25 µg KLH), INP#3 for three weeks. Starting from the 21st day, all the mice were immunized with IV injection of free KLH (50 µg) for three weeks (one dose per week). The mice sera were collected on the day of 21st, 28th, and 35th (right before the antigen immunization) for antibody detection via ELISA test.

### **3.6 ELISA**

The mouse sera were collected for ELISA test to determine the production of antigen-specific Abs. As the first step of direct ELISA test of anti-KLH Abs, 100 µL KLH solutions (10 µg/mL) prepared in coating buffer (0.1 M sodium carbonate buffer, pH 10.5) were used to coat each well of 96-well plates. After overnight coating at 4 °C, the plates were washed five times using washing buffer (0.05% Tween 20 in PBS buffer) to remove the KLH solutions and then filled with blocking buffer (1% BSA solution in 0.1 M Tris buffer, pH 8.0) for 1-h incubation at room temperature, after which the blocking buffer was removed. All wells were then washed by washing buffer for another five times. Subsequently, serial dilutions of mice sera in PBS buffer containing 1% BSA were added to the plates (100 µL/well) for 2-h incubation at 37 °C, after which the mice sera were removed and all wells were washed five times with PBS buffer. Next, goat anti-mice IgG (HRP-conjugated) as the secondary antibody was added into each well for

another 1-h incubation at room temperature. Subsequently, all the wells were washed five times using washing buffer before the addition of 100  $\mu$ L/well HRP substrate 3,3',5,5'-tetramethylbenzidine (TMB). The plates were shaken for 15 min, and 100  $\mu$ L stop solution (0.2 M H<sub>2</sub>SO<sub>4</sub>) was added to each well. OD value at 450 (signal) and 570 nm (background) was recorded by a microplate reader. Mice sera naïve to the administration of KLH proteins were used as the negative control for all ELISA detections.

## 4. Result and discussion

### 4.1 Size distribution and zeta-potential of immunosuppressive nanoparticles

The dynamic light scattering (DLS) result in Figure 3 showed a uniform hydrodynamic size of INPs (35.1 nm, PDI 0.24). In general, chromatin complex was composed by DNA and proteins. DNA wraps around histone proteins to form nucleosomes and then multiple histones wrap into a 30-nm chromatin which compact multiple nucleosome arrays. The size of INPs indicated the zwitterionic material-based nanoparticles as a suitable chromatin-mimetic unit. Moreover, smaller NPs (1-10 nm) are associated with the tendency to be cleared rapidly from the body via renal filtration and urinary excretion. Increasing the hydrodynamic size of NPs can decrease rapid renal clearance and prolong the circulation time of NPs. Here, the size of INPs can avoid rapid renal clearance.

The zeta potential measurement by Malvern zetasizer showed that the INPs were positive charged (+19.5mV) (Figure 4). In the INPs formulation, payloads (GpG and KLH) were negatively charged, while tbCB was positively charged. The electrostatic interaction between

positively charged tbCB and negatively charged GpG/KLH also contributed to the stability of INPs. Hence, the overall positive charge of INPs also indicated a stable formulation to constrain GpG and KLH successfully in INPs. Moreover, this indicated that for the specific formulation (GpG:KLH = 8:1, Monomers:GpG = 3200:1), the surface charge of INPs was preferred for APC uptake. Prior studies have demonstrated the effect of nanoparticle surface charge on cell uptake. Specifically, cationic nanoparticles can be preferentially internalized by APCs due to electrostatic interaction with anionic cell membranes. Due to the incorporation of a cationic CB ester, INP encapsulation could induce a higher payload uptake by APCs than non-encapsulated payload.

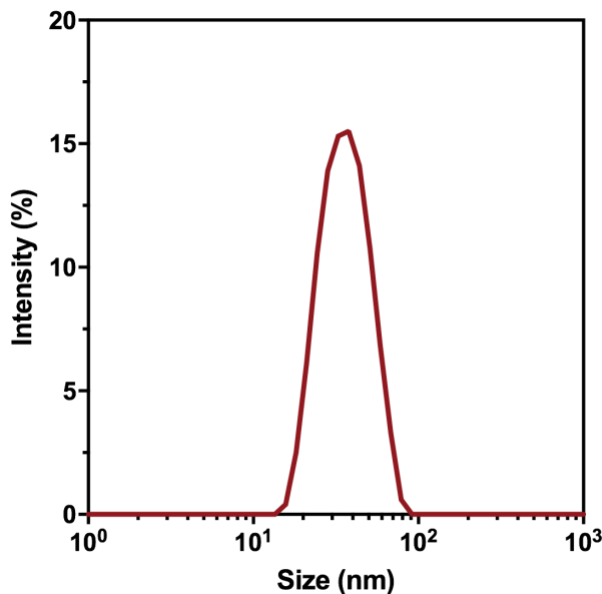


**Figure 3. Size distribution of INPs characterized by Malvern Zetasizer.**

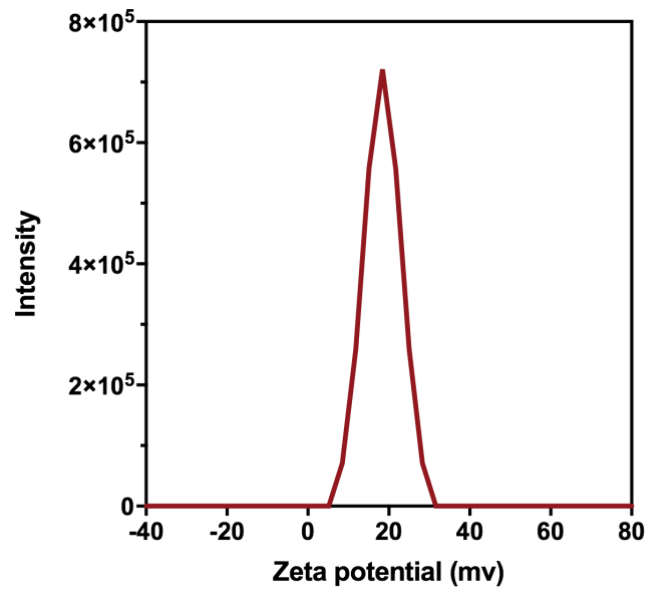


**Figure 4. Zeta potential of INPs characterized by Malvern Zetasizer.**

#### **4.2 Optimize the encapsulation result**

Recent reports have demonstrated that the co-administration of immunosuppressive regulatory signals and antigens (self-molecules in autoimmune disease or environmental allergens in allergies) can promote antigen-specific tolerance. However, the delivery of regulatory signals without aim antigen will cause non-antigen-specific immune tolerance, which increases infectious susceptibility. Without co-delivery with regulatory signals, over-exposure of antigen will induce inflammation. Addressing these problems, a nanoparticle carrier is expected to possess the ability of bearing both components and releasing the payloads directly into cells of interest, thus avoiding off target effects present in co-delivery without a nanoparticle carrier. Here, we constructed the INPs to achieve co-delivery of antigen (KLH) and immunosuppressive regulatory signal (GpG). GpG and KLH were encapsulated into INPs with tunable ratios. The

INPs were designed to be sufficiently stable under neutral conditions, but dissociative under the endosomal pH. The INP carrier can effectively carry negatively-charged GpG through electrostatic interaction with cationic tbCB. In the meantime, KLH was encapsulated inside the INPs upon gelation between cross-linker, AAm and tbCB. To prove that INPs could successfully co-encapsulate GpG and KLH, a novel method was applied in this thesis.

Agarose gel electrophoresis is typically used in molecular biology to separate DNA or RNA molecules by their size. The size-based separation is achieved by driving negatively charged nucleic acid molecules through the agarose matrix with an electronic field. There are several factors that affect the migration of nucleic acid bands. The most important factor is molecular weight of DNA or RNA. Smaller nucleic acid molecules with shorter length will move faster and migrate farther through agarose gel. However, longer nucleic acid molecules with higher molecular weight will travel slower due to the hindrance by gel matrix. This method can be used to estimate the size of DNA molecules when used with a standard DNA ladder, analyze the quality and purity of PCR products, or separate genomic DNA for further analysis. Secondly, voltage can affect the migration of bands. Using higher voltage will lead to faster migration of DNA or RNA. However, this will also increase the temperature and even cause the gel to melt. 100mV is typically used in DNA separation. Thirdly, agarose gel density can affect the migration speed and the separation quality. Usually, agarose gel can be used to separate DNA fragments from 50 base pair to millions of bases. Increase the agarose concentration will increase the gel density and decrease the mesh size of the gel, which reduce the migration speed and enable the separation of smaller nucleic acid molecules. In general, lower concentrations of agarose gel can be more suitable for larger molecules, so that they will not get stuck at the start position of the

gel. 1% gels are commonly used for many applications, and here we used 2% gels for a better resolution.

To visualize GpG and KLH simultaneously in the agarose gel, different fluorescent labels were applied. Most commonly used method to stain proteins in gel electrophoresis is using the non-fluorescent dye Coomassie Brilliant Blue. The dye interacts electrostatically but noncovalently with the amino and carboxyl groups of proteins to form a protein–dye complex for visualization. However, the staining process is time consuming and the resolution is limited. EtBr is a common fluorescent tag for nucleic acid in agarose gel electrophoresis. When exposed to UV light, it will fluoresce intensively after binding to DNA. By moving into the hydrophobic environment between the base pairs of DNA and away from the solvent, EtBr is able to shed any water molecules around it. As water is a highly efficient fluorescent quencher, the removal of water molecules allows EtBr to fluoresce. In this thesis, we reported a novel strategy to visualize DNA and protein simultaneously. EtBr was used for agarose gel preparation to stain GpG. Rhodamine was used to label KLH. Since the absorption and excitation spectrums of Rhodamine 6G and EtBr overlap with each other, the band of GpG and Rhodamine-labeled KLH can be simultaneously observed by imaging of agarose gel electrophoresis.

Here, Successful encapsulation was determined by gel electrophoresis (Figure 5). The M:G ratio was tuned to allow complete encapsulation of GpG and KLH. The size of KLH and GPG encapsulated INPs was larger than the mesh size of 2 % agarose gel, which will inhibit the migration of INPs through the agarose gel. For well 1 (M:G ratio = 6400:1) and well 2 (M:G ratio = 3200:1), the bands stayed in the well without migration, which indicated that KLH and GpG

were both fully encapsulated in INPs. For well 3 (M:G ratio = 1600:1), the band was only partially staying in the well. The clear band which migrated to same position of free-KLH indicated that this formulation was not able to fully encapsulate KLH within the INPs. For well 4 (M:G ratio = 800:1), another band which migrated to the same position of free GpG indicated that there were free GpG in this formulation. For the following formulations (M:G ratio < 1600:1), most of the GpG and KLH migrated away from the well. This was because the limited number of cationic monomer and gelation in these formulations was not able to trap GpG and protein within the INPs. In order to achieve co-delivery of GpG and KLH, we chose first two formulations for further study. In conclusion, the INP carrier with higher M:G ratio (6400:1 and 3200:1) can effectively carry negatively-charged GpG and encapsulate KLH, thus deliver the payloads simultaneously.

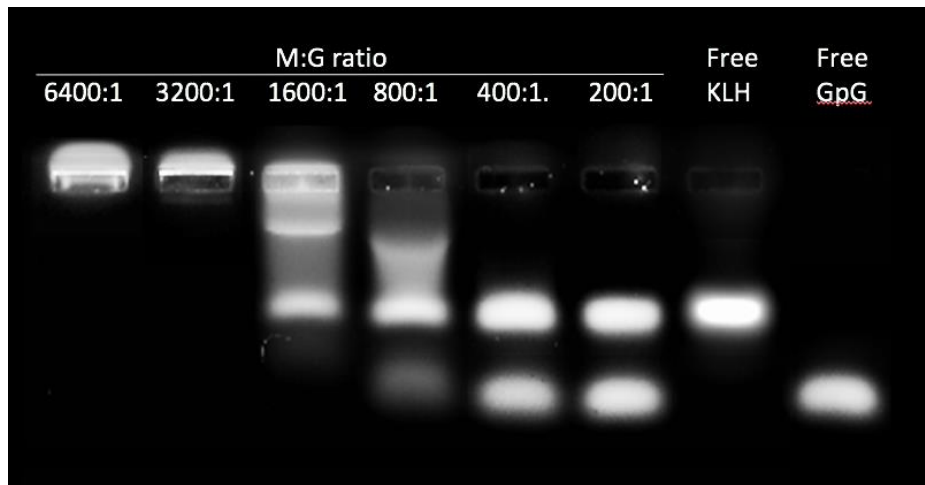


**Figure 5. Optimize of the formulation of INPs.** Agarose gel electrophoresis of INPs synthesized with a fixed weight ratio of GpG to KLH (G:K= 8:1) but varied monomer to GpG (M:G) molar ratios (200:1, 400:1, 800:1, 1600:1, 3200:1, 6400:1).

### 4.3 Stability test

Stability test of INPs (M:G molar ratio = 6400:1) was carried out in both PBS solution and heparin solution. PBS solution provided the physiological condition (pH 7.4), yet heparin competition assay was applied to challenge the DNA trapping ability of INPs. Heparin assays were commonly utilized to mimic the circulation for nucleic acid delivery. As a polyanion existing in serum, heparin can compete with DNA and bind to cationic nanoparticles via electrostatic interaction. For the nanoparticles which the nucleic acid payloads were assembled merely via electrostatic interaction, heparin binding can decrease the stability of the nanoparticles and cause pre-releasing of the nucleic acid payload. To prove the stability of INPs in blood circulation, heparin was applied to compete with DNA binding and challenge the stability of INPs. The heparin concentration in human plasma is 1 to 2.4 mg per liter. Here, to test the ability of INPs to resist Heparin binding, competing assays were carried out with different concentrations of Heparin (5 mg/ml and 15 mg/ml), both concentrations were higher than heparin concentration in human plasma.

As shown in Figure 6, INPs incubated with PBS and heparin solution stayed in the loading well without visible releasing of GpG or KLH, even in the presence of the higher concentration of Heparin. This indicated that the cationic tbCB and cross-linking mesh in INPs could provide a stable interaction of GpG and KLH, which benefited the co-delivery of antigen and immunosuppressive molecule to induce antigen-specific immune tolerance.



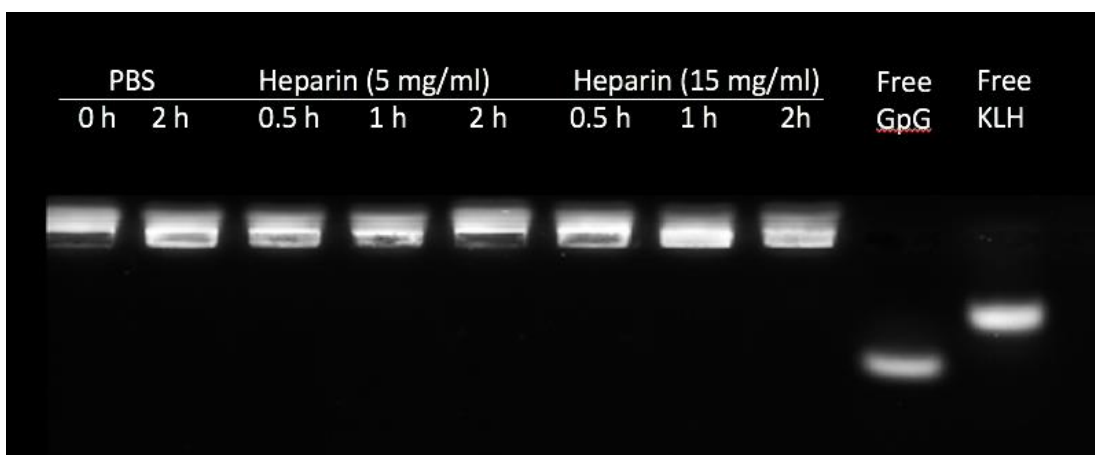


**Figure 6. The stability of INPs in physiological condition and Heparin competing assay.**

The INPs were stable without releasing free GpG and KLH for 2 hours.

#### 4.4 Degradation test

The *in vivo* use of non-degradable NPs is debatable regarding safety concerns. Without efficient degradation which promotes further elimination out of the body, such non-degradable NPs can accumulate in the MPS organs, and cause potential toxicity. Degradable NPs are more applicable for the aim of drug delivery. The ability to be chemically broken down into biocompatible small molecules is strongly associated with the metabolism and excretion of NPs and is highly emphasized for NP related clinical trials. The most common design of degradable drug-loaded NPs is based on drug releasing upon the degradation of NPs. The degradation can be triggered upon hydrolysis or achieved by inducing pH-sensitive bond, ROS responsive linkers, or glutathione responsive linkers.

In this thesis, the INPs was cross-linked by acid-degradable crosslinker glycerol diamethacrylate, which was stable under neutral pH and degradable in acidic environment. The degradation profile of INPs was examined under endosomal pH (pH = 5.4). As shown in figure 7, in the first lane, fresh-prepared INPs stayed in the loading well which indicated a stable encapsulation of GpG and KLH. Under the incubation at endosomal pH, the content of KLH was firstly released from the INPs as shown by the migrated band that began to appear after 1h (well 3). This indicated that the acidic condition could induce the degradation of INPs, favoring the release of encased protein antigens into endosomal compartments. After 2-hour incubation, the migrated band representing the released GpG became visible, confirming the reversion of cationic tbCB to zwitterionic PCB as well as the degradation of INPs could also efficiently promote the unpackaging of GpG. Furthermore, the disappearance of the original band representing INPs in the gel electrophoresis implied that most of the GpG and KLH encapsulated within INPs could be released within 4 hours, which is sufficient to allow them to be fully released in the endosomal environment.

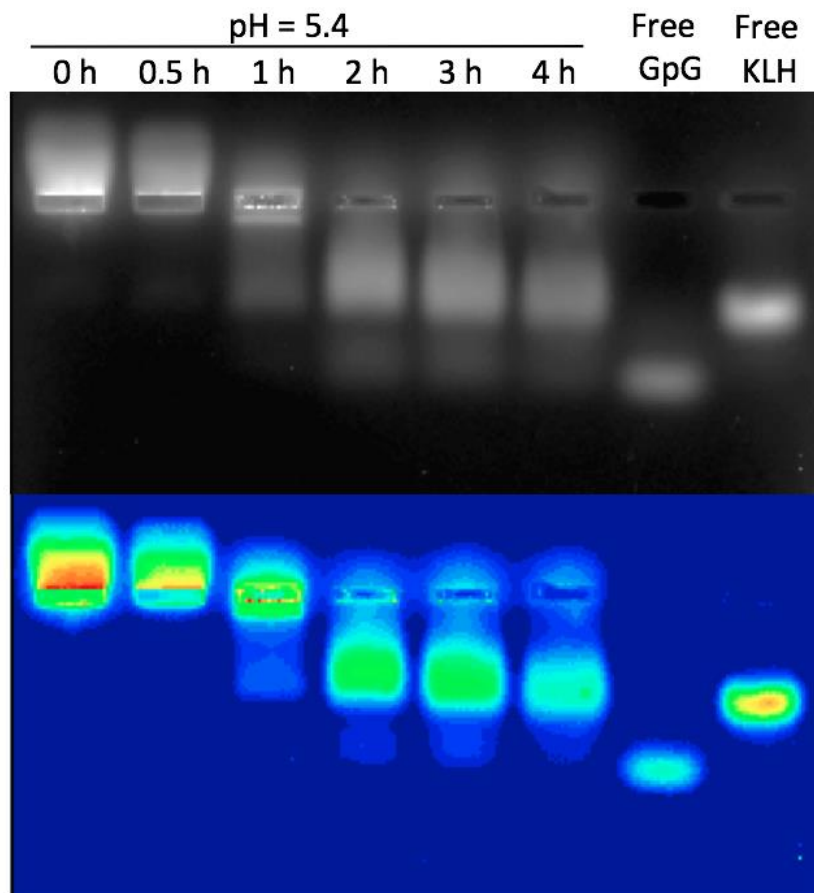


**Figure 7. Degradation study of INPs at pH = 5.4.**

#### 4.5 Immune modulation result

As illustrated in Figure 8, mice were IV. injected weekly with: (i) free KLH alone (50 µg) for eight weeks (control 1); (ii) PBS (control 2) or three INPs formulations containing (#1: 50 µg KLH/ 12.5 µg GpG; #2: 50 µg KLH/ 50 µg GpG; #3: 50 µg KLH/ 200 µg GpG) for the first three weeks, followed by three weekly challenges of free KLH (50 µg) starting from day 21. The mice sera were collected on day 14, 21, 28 and 35 for Ab detection via ELISA test.

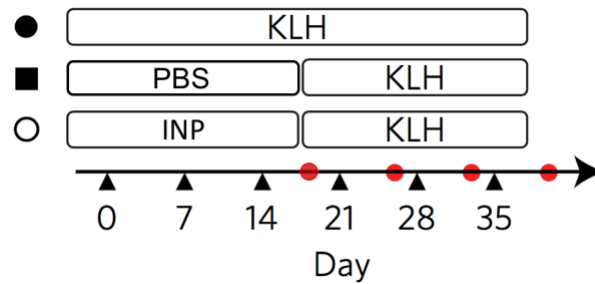


**Figure 8. Scheme of KLH tolerance study.** Mice were IV injected weekly with: (i) KLH, (ii) PBS, (iii) INP with three different formulations (INP#1, #2, #3) for the first three weeks, followed by three weekly challenges of free KLH starting from 21st day. The mice sera were collected on the 21st, 28th, 35<sup>th</sup> day for Ab detection via ELISA test.

To assess whether INPs could induce immunological tolerance to co-delivered protein antigen, and not just transient unspecific immunosuppression, mice were treated with three intravenous injections of KLH, a highly immunogenic antigen, and then repeated challenged with KLH alone (Figure 9). Apparently, INP#1 that contain the least amount of GpG displayed limited effect in the reduction of anti-KLH Abs. In contrast, mice treated with INP#2 showed an over 100-fold reduction in titers compared with control groups that received KLH alone. Moreover, three IV. injections of INP#3 of GpG could utterly inhibit the generation of anti-KLH Abs even after being challenged by five weekly doses of free KLH. The difference in magnitude of KLH-

specific immune responses suggest that the dose of GpG plays a critical role in producing a complete immunological tolerance. Moreover, the PBS-treated group, as a delayed-immunization control group, showed a robust antibody response to the challenge of free KLH, indicating that the efficacy of INP treatment resulted in a sustained immunological tolerance and not simply a delayed response stemmed from the INP-shell protection.

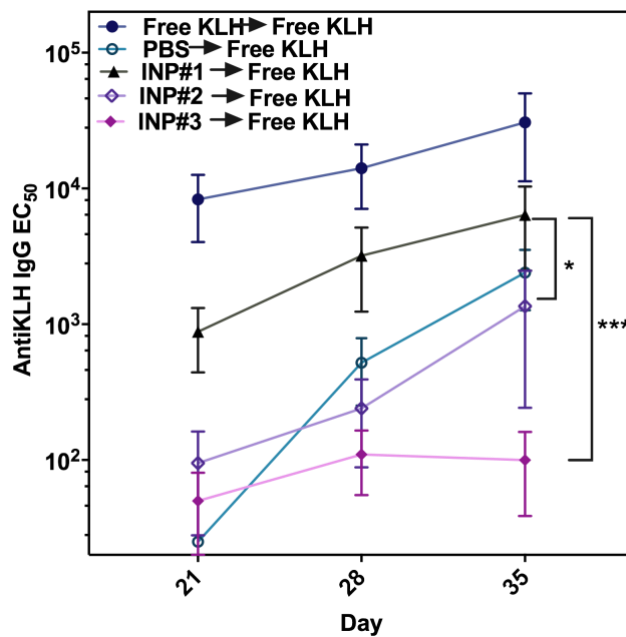


**Figure 9. Time course of anti-KLH IgG antibody development in mice sera.**

## Conclusions

This thesis developed a zwitterionic-switchable INP as a new approach to eliminate the undesirable immune responses to a specific protein antigen by inducing immunological tolerance. Such an INP was designed to stably encase GpG, an immunosuppressive nucleotide, and protein antigens under physiological condition, but switch to release cargos under acidic endosomal condition. The formulation of INPs was also characterized and optimized in terms of stability and degradability. Moreover, the intravenous pre-treatment of INPs containing KLH was shown to induce a durable immunological tolerance to KLH, which is resistant to immunogenic challenges by KLH for at least three weeks. This INP as a safe and efficient tool capable of inducing antigen-specific immune tolerance is expected to find a wide range of applications in various clinical scenarios, including protein drug therapies, autoimmune disease, rejection of transplanted cells, and allergies.

## Reference

1. Krieckaert C, Rispens T, & Wolbink G (2012) Immunogenicity of biological therapeutics: from assay to patient. *Curr Opin Rheumatol* 24(3):306-311.
2. Nechansky A & Kircheis R (2010) Immunogenicity of therapeutics: a matter of efficacy and safety. *Expert Opin Drug Dis* 5(11):1067-1079.
3. Chirmule N, Jawa V, & Meibohm B (2012) Immunogenicity to Therapeutic Proteins: Impact on PK/PD and Efficacy. *Aaps J* 14(2):296-302.
4. Godsel LM, *et al.* (2001) Prevention of autoimmune myocarditis through the induction of antigen-specific peripheral immune tolerance. *Circulation* 103(12):1709-1714.
5. Kontos S, Grimm AJ, & Hubbell JA (2015) Engineering antigen-specific immunological tolerance. *Curr Opin Immunol* 35:80-88.
6. Maldonado RA, *et al.* (2015) Polymeric synthetic nanoparticles for the induction of antigen-specific immunological tolerance. *P Natl Acad Sci USA* 112(2):E156-E165.
7. Kishimoto TK, *et al.* (2016) Improving the efficacy and safety of biologic drugs with tolerogenic nanoparticles. *Nat Nanotechnol* 11(10):890-+.
8. Fabian MC, Lakey JRT, Rajotte RV, & Kneteman NM (1993) The Efficacy and Toxicity of Rapamycin in Murine Islet Transplantation - in-Vitro and in-Vivo Studies. *Transplantation* 56(5):1137-1142.
9. Whiting PH, *et al.* (1991) Toxicity of Rapamycin - a Comparative and Combination Study with Cyclosporine at Immunotherapeutic Dosage in the Rat. *Transplantation* 52(2):203-208.
10. Anonymous (2005) Pulmonary toxicity associated with rapamycin in a pediatric renal transplant patient. *Clin Toxicol* 43(6):655-656.
11. Marti HP & Frey FJ (2005) Nephrotoxicity of rapamycin: an emerging problem in clinical medicine. *Nephrol Dial Transpl* 20(1):13-15.
12. Ferguson TA, Choi JY, & Green DR (2011) Armed response: how dying cells influence T-cell functions. *Immunol Rev* 241:77-88.
13. Griffith TS & Ferguson TA (2011) Cell Death in the Maintenance and Abrogation of Tolerance: The Five Ws of Dying Cells. *Immunity* 35(4):456-466.
14. Yatim N, Cullen S, & Albert ML (2017) Dying cells actively regulate adaptive immune responses. *Nat Rev Immunol* 17(4):262-275.
15. Liu K, *et al.* (2002) Immune tolerance after delivery of dying cells to dendritic cells in situ. *J Exp Med* 196(8):1091-1097.
16. Miles K, *et al.* (2012) A tolerogenic role for Toll-like receptor 9 is revealed by B-cell interaction with DNA complexes expressed on apoptotic cells. *P Natl Acad Sci USA* 109(3):887-892.
17. Zhu FG, Reich CF, & Pisetsky DS (2002) Inhibition of murine dendritic cell activation by synthetic phosphorothioate oligodeoxynucleotides. *J Leukoc Biol* 72(6):1154-1163.
18. Ho PP, *et al.* (2005) A suppressive oligodeoxynucleotide enhances the efficacy of myelin cocktail/IL-4-tolerizing DNA vaccination and treats autoimmune disease. *J Immunol* 175(9):6226-6234.
19. Barrat FJ & Coffman RL (2008) Development of TLR inhibitors for the treatment of autoimmune diseases. *Immunol Rev* 223:271-283.
20. Tostanoski LH, *et al.* (2016) Design of Polyelectrolyte Multilayers to Promote Immunological Tolerance. *ACS Nano*.

21. Ho PP, Fontoura P, Ruiz PJ, Steinman L, & Garren H (2003) An immunomodulatory GpG oligonucleotide for the treatment of autoimmunity via the innate and adaptive immune systems. *J Immunol* 171(9):4920-4926.
22. Conroy H, Marshall NA, & Mills KH (2008) TLR ligand suppression or enhancement of Treg cells? A double-edged sword in immunity to tumours. *Oncogene* 27(2):168-180.
23. Sun S, Rao NL, Venable J, Thurmond R, & Karlsson L (2007) TLR7/9 antagonists as therapeutics for immune-mediated inflammatory disorders. *Inflamm Allergy Drug Targets* 6(4):223-235.
24. Mills KH (2008) TLR9 turns the tide on Treg cells. *Immunity* 29(4):518-520.
25. Zhang Z, *et al.* (2008) The hydrolysis of cationic polycarboxybetaine esters to zwitterionic polycarboxybetaines with controlled properties. *Biomaterials* 29(36):4719-4725.
26. Sinclair A, *et al.* (2013) Engineering Buffering and Hydrolytic or Photolabile Charge Shifting in a Polycarboxybetaine Ester Gene Delivery Platform. *Biomacromolecules* 14(5):1587-1593.
27. Zhang L, *et al.* (2013) Hydrolytic Cationic Ester Microparticles for Highly Efficient DNA Vaccine Delivery. *Small* 9(20):3439-3444.
28. Cao ZQ & Jiang SY (2012) Super-hydrophilic zwitterionic poly(carboxybetaine) and amphiphilic non-ionic poly(ethylene glycol) for stealth nanoparticles. *Nano Today* 7(5):404-413.
29. Li B, *et al.* (2018) Mitigation of Inflammatory Immune Responses with Hydrophilic Nanoparticles. *Angew Chem Int Ed Engl.*
30. Li B, *et al.* (2018) Zwitterionic Nanocages Overcome the Efficacy Loss of Biologic Drugs. *Adv Mater.*
31. Zhang L, *et al.* (2013) Zwitterionic hydrogels implanted in mice resist the foreign-body reaction. *Nat Biotechnol* 31(6):553-+.
32. Zhang P, *et al.* (2015) Zwitterionic gel encapsulation promotes protein stability, enhances pharmacokinetics, and reduces immunogenicity. *P Natl Acad Sci USA* 112(39):12046-12051.
33. Carbone J, del Pozo N, Gallego A, & Sarmiento E (2011) Immunological risk factors for infection after immunosuppressive and biologic therapies. *Expert Rev Anti-Infe* 9(4):405-413.
34. Riminton DS, Hartung HP, & Reddel SW (2011) Managing the risks of immunosuppression. *Curr Opin Neurol* 24(3):217-223.